

Evidence of competing s and d -wave pairing channels in iron-based superconductors

F. Kretzschmar,¹ B. Muschler,¹ T. Böhm,¹ A. Baum,¹ R. Hackl,¹
 Hai-Hu Wen,² V. Tsurkan,^{3,4} J. Deisenhofer,³ and A. Loidl³

¹Walther Meissner Institute, Bavarian Academy of Sciences and Humanities, 85748 Garching, Germany

²Nanjing University, Nanjing, P.R. China

³Experimental Physics 5, Center for Electronic Correlations and Magnetism,
 Institute of Physics, University of Augsburg, 86159 Augsburg, Germany

⁴Institute of Applied Physics, Academy of Sciences of Moldova, MD-2028, Chisinau, Republic of Moldova

(Dated: December 3, 2024)

We show that electronic Raman scattering affords a window into the essential properties of the pairing potential $V_{\mathbf{k},\mathbf{k}'}$ of iron-based superconductors. In $\text{Ba}_{0.6}\text{K}_{0.4}\text{Fe}_2\text{As}_2$ we observe band dependent energy gaps along with excitonic Bardasis-Schrieffer modes characterizing, respectively, the dominant and subdominant pairing channel. The $d_{x^2-y^2}$ symmetry of all excitons allows us to identify the subdominant channel to originate from the interaction between the electron bands. Consequently, the dominant channel driving superconductivity results from the interaction between the electron and hole bands and has the full lattice symmetry. The results in $\text{Rb}_{0.8}\text{Fe}_{1.6}\text{Se}_2$ along with earlier ones in $\text{Ba}(\text{Fe}_{0.939}\text{Co}_{0.061})_2\text{As}_2$ highlight the influence of the Fermi surface topology on the pairing interactions.

PACS numbers: 78.30.-j, 74.72.-h, 74.20.Mn, 74.25.Gz

INTRODUCTION

Cooper pairing in superconductors is driven by the interaction potential $V_{\mathbf{k},\mathbf{k}'}$ between two electrons. In conventional superconductors with an isotropic gap Δ prominent structures appear in many spectroscopies at $\hbar\omega_{\mathbf{q}} + \Delta$, and $V_{\mathbf{k},\mathbf{k}'}$ can be derived by and large from the spectrum of interactions $\hbar\omega_{\mathbf{q}}$ [1]. This access is hampered in systems with the gap $\Delta_{\mathbf{k}}$ varying strongly with the electronic momentum $\hbar\mathbf{k}$. The iron-based superconductors [2, 3], as shown in Fig. 1, open up new vistas. Since the hole- and electron-like Fermi surfaces can be tuned by substitution [Fig. 1(c) and (d)] they can be considered model systems for studying the pairing interaction in anisotropic multi-band systems [4–6]. Repulsive spin [7] and attractive orbital [8] fluctuations were suggested to provide appreciable interaction potentials $V_{\mathbf{k},\mathbf{k}'}$. The resulting ground states may preserve [Fig. 1(e)] or break the full lattice symmetry [Fig. 1(f)]. In the spin channel, the interactions between either the central hole-like and the peripheral electron-like Fermi surfaces V_s [7] or the electron bands alone V_d are nearly degenerate [5, 9] [Fig. 1(c) and (d)] and entail a sign change of the energy gap $\Delta_{\mathbf{k}}$ [Fig. 1(e) and (f)].

Raman scattering offers an opportunity to scrutinize competing superconducting instabilities and derive essential properties of $V_{\mathbf{k},\mathbf{k}'}$. The electronic response provides direct access to the energy gap and its momentum dependence [10, 11] reflecting the dominant channel responsible for Cooper pairing. In addition, residual interactions resulting from anisotropies of the pairing potential $V_{\mathbf{k},\mathbf{k}'}$ may lead to sharp in-gap modes due to the formation of bound states of the two electrons of a broken Cooper pair [9, 12–15] similar to electron-hole excitons in semiconduc-

tors. The energy and the symmetry properties of these “Cooperons” provide insight into the momentum dependence of $V_{\mathbf{k},\mathbf{k}'}$ or decompositions thereof in terms of orthonormal functions ϕ_i such as $V_{\mathbf{k},\mathbf{k}'} = \phi_s^2 V_s + \phi_d^2 V_d + \dots$ and, consequently, the type of interaction.

In this paper, we present light scattering spectra as a function of the Fermi surface topology in order to gain insight into the pairing interaction. The results on the electron-doped iron-chalcogenide $\text{Rb}_{0.8}\text{Fe}_{1.6}\text{Se}_2$ and the hole-doped iron-pnictide $\text{Ba}_{0.6}\text{K}_{0.4}\text{Fe}_2\text{As}_2$ are analyzed along with the data of $\text{Ba}(\text{Fe}_{0.939}\text{Co}_{0.061})_2\text{As}_2$ studied earlier [20].

SAMPLES

The optimally doped $\text{Ba}_{0.6}\text{K}_{0.4}\text{Fe}_2\text{As}_2$ single crystals were grown with the self-flux method [21]. The x-ray diffraction patterns taken on these samples show only [00l] peaks and very good crystallinity. Specific heat measurements reveal a residual coefficient γ_0 of about 1 mJ/mol K², indicating a very clean sample. The resistivity curve shows that the transition starts at about 39.0 K, and ends at about 38.5 K, which is consistent with a very sharp magnetic transition.

We studied two different single crystals. As can be seen in Fig. 2 the spectra are well reproducible concerning the overall intensity and the major part of the spectral shape. A closer look reveals small differences. The phonon line at 180 cm⁻¹ [Fig. 2(a)] and the superconductivity-induced structures at 140 and 170 cm⁻¹ [Fig. 2(b)] are a little more intense in sample 1 than in sample 2 indicating a slightly smaller impurity concentration in sample 1. For this reason we show the results from sample 1 in the paper.

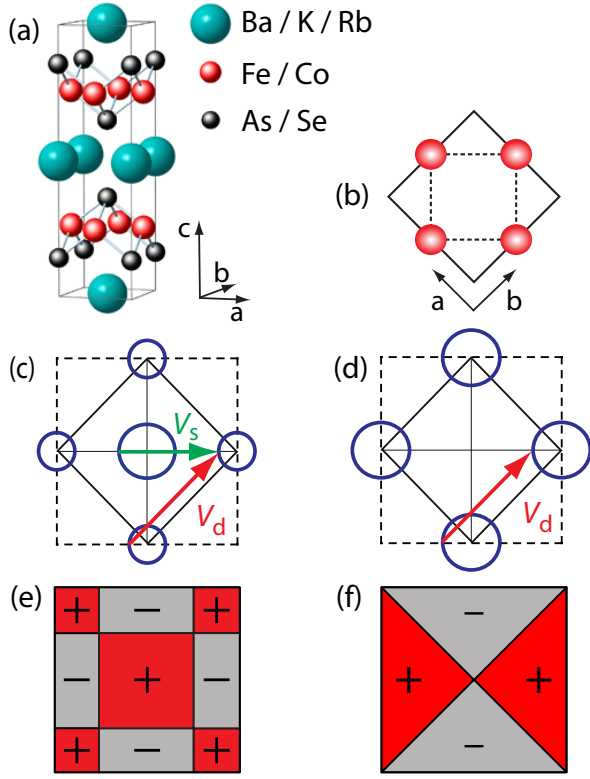


FIG. 1. (Color online) Crystal and reciprocal lattices of iron-based superconductors. (a) FeAs/Se layers (small spheres) and (earth) alkali metals (big spheres). (b) 1 Fe unit cell. (c), (d) First Brillouin zones (BZ, dashes for the 1 Fe cell) with schematic Fermi surfaces of (c), $\text{Ba}_{0.6}\text{K}_{0.4}\text{Fe}_2\text{As}_2$ [16, 17] and (d), $\text{Rb}_{0.8}\text{Fe}_{1.6}\text{Se}_2$ [18, 19]. Also indicated are the two dominant interaction potentials V_s and V_d . (e) For $V_s > V_d$ the pairing state is predicted to have s_{\pm} symmetry for which the phase of the gap on the hole and electron bands differs by π [6, 7]. (f) For $V_d > V_s$ a state with $d_{x^2-y^2}$ symmetry is favored [5, 9].

$\text{Rb}_{0.8}\text{Fe}_{1.6}\text{Se}_2$ single crystals were prepared by the Bridgman method. Polycrystalline FeSe synthesized from the high-purity elements (99.98 % Fe and 99.999 % Se and 99.75 % Rb) were used as starting materials. Handling of the reaction mixtures was done in an argon box with residual oxygen and water content less than 1 ppm. The composition of the grown samples was determined by wavelength dispersive spectroscopy (WDS) using the electron probe micro-analyzer (EPMA) Cameca SX50 with an accuracy of 0.5 % for Fe and 1 % for Se. The sharp superconducting transition with an onset temperature of 32.4 K was evidenced by susceptibility and specific heat measurements. The preparation and characterization details of the samples investigated here (BR16) are given in Ref. [22]. Recently, evidence was reported that $\text{Rb}_{0.8}\text{Fe}_{1.6}\text{Se}_2$ is a system with macroscopically phase-separated antiferromagnetic insulating and metallic (superconducting) layers [23–25]. However, both the well defined \mathbf{Q} vectors of the spin resonance in neutron scat-

tering [26] and the selection rules in our light scattering experiments show that the different layers are correlated and uniquely oriented.

The influence of this layered structure on the light scattering experiments is expected to be weak since only the metallic (superconducting) part contributes to the particle-hole continuum. It turns out that the scattering intensity from all samples studied here is comparable. This is an indication that the absorption of the light is weak in the insulating layers and that scattering volume is similar in all samples studied. In contrast to the continuum, scattering from phonons may also come from the insulating part. The large number of phonons has its origin in the low symmetry of the crystals induced by Fe and Rb vacancies.

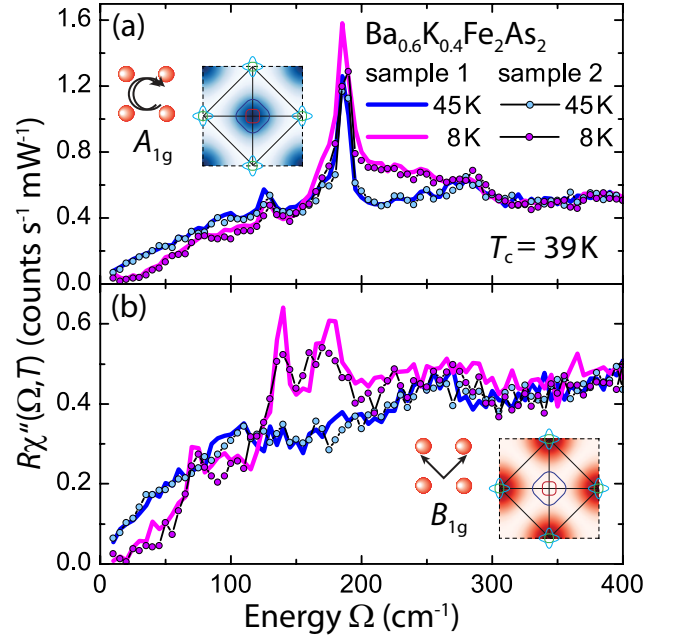


FIG. 2. (Color online) Comparison of the spectra of two different single crystals of $\text{Ba}_{0.6}\text{K}_{0.4}\text{Fe}_2\text{As}_2$ (raw data). Without adjustment all electronic intensities coincide.

EXPERIMENT

The experiments were performed with standard light scattering equipment. The figures display the Raman susceptibilities $R\chi''_{\gamma,\gamma}(\Omega, T) = S(\Omega, T)\{1 + n(T, \Omega)\}^{-1}$ where R is an experimental constant, S is the van Hove function being proportional to the rate of scattered photons, and n is the Bose-Einstein distribution. The polarizations of the incoming and scattered photons are given with respect to the 1 Fe unit cell [Fig. 1 (b)] relevant for the electronic properties. The related excitation symmetries translate into sensitivities in momentum space for electron-hole excitations [11] as shown in the insets of

Figs. 3 and 4. The symmetry properties of the collective modes reflect those of the subdominant channels in the potential $V_{\mathbf{k},\mathbf{k}'}$ which do not support pairing in the ground state [14].

RESULTS

The symmetry-dependent Raman response of $\text{Rb}_{0.8}\text{Fe}_{1.6}\text{Se}_2$ is shown in Fig. 3. Due to surface issues there is a relatively strong increase towards the laser line. In the A_{1g} and B_{2g} spectra, the relative difference between the normal and the superconducting state is weak and absent, respectively, since the band structure of $\text{Rb}_{0.8}\text{Fe}_{1.6}\text{Se}_2$ [18, 19] does not have Fermi surface crossings close to the sensitivity maxima of the related form factors (see insets of Fig. 3). In B_{1g} symmetry, the suppression of the low-temperature spectra due to the gap and the excess intensity at and above 2Δ can be considered a typical features of a superconductor [11]. The relative changes of below and above a threshold at approximately 60 cm^{-1} reach 80 and 30%, respectively [Fig. 3(c)]. Below 60 cm^{-1} , the intensity is only weakly energy dependent indicating a clean isotropic gap. The phonons at 80 and 115 cm^{-1} , close to the gap edge, gain intensity below T_c as expected for weak electron-phonon coupling. As can be seen directly in the insets of Fig. 3 an appreciable response is expected only in B_{1g} symmetry if hole-like bands in the Brillouin zone center are absent. In the presence of hole bands, gap structures appear also in A_{1g} symmetry [20]. Hence, the selection rules based on symmetry arguments corresponding to the 1 Fe unit cell [20] are supported by the results in $\text{Rb}_{0.8}\text{Fe}_{1.6}\text{Se}_2$ and are likely to be of general significance in the iron-based superconductors.

In Fig. 4, we show Raman spectra of $\text{Ba}_{0.6}\text{K}_{0.4}\text{Fe}_2\text{As}_2$. Here, we observe superconductivity-induced features in all symmetries. Below a symmetry independent threshold of approximately 25 cm^{-1} the response is very small and nearly energy independent. Although the intensity is not exactly zero it is safe to conclude that there is a full gap on all bands having a magnitude of at least $0.9 k_B T_c$. The excess intensity in the range $130 < \Omega < 300\text{ cm}^{-1}$ originates from either pair-breaking [Fig. 4(a) and (b)] or, as will be discussed in detail below, from collective excitations [Fig. 4(c)]. The spectral features in A_{1g} and B_{2g} symmetry [Fig. 4(a) and (b)] are broad and asymmetric whereas the peaks in B_{1g} symmetry [Fig. 4(c)] are rather sharp and symmetric. The important secondary structures of the spectra between the minimal and the maximal gaps are better resolved in the difference spectra in panel (d) of Fig. 4. In this way, the contributions from phonons are by and large subtracted out. Only the Fe vibration at 215 cm^{-1} in the B_{2g} spectrum (B_{1g} phonon in the crystallographic cell) has an anomalous intensity for its proximity to the gap edge and is truncated. Both

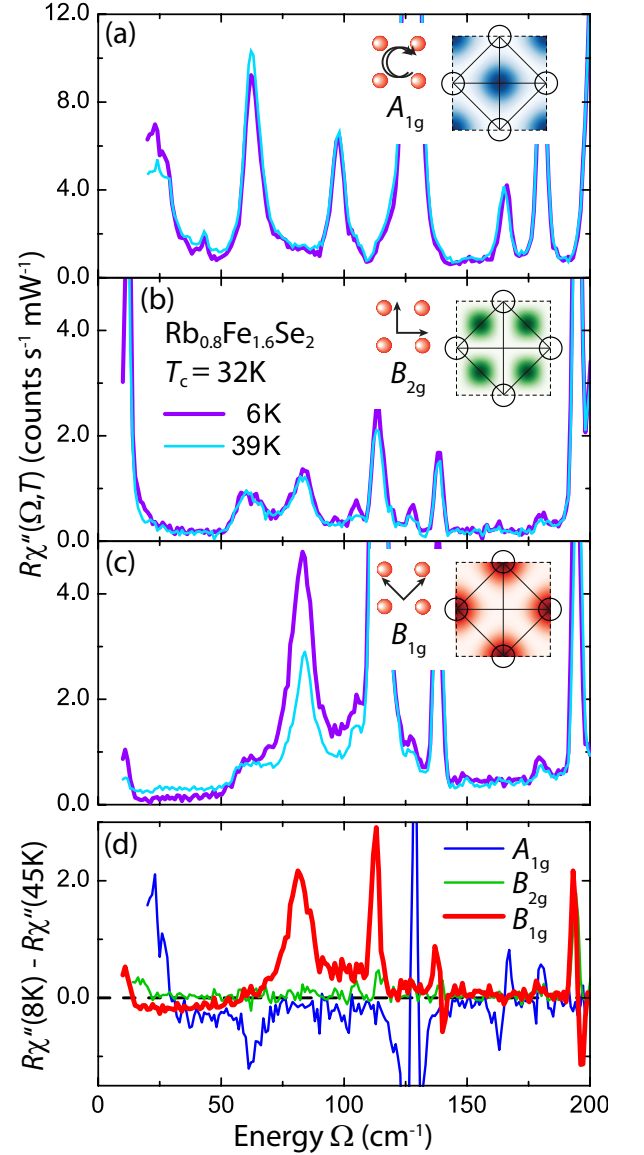


FIG. 3. (Color online) Normal and superconducting Raman spectra of $\text{Rb}_{0.8}\text{Fe}_{1.6}\text{Se}_2$ at temperatures as indicated. The insets show the correspondence between light polarizations and sensitivities in momentum space for the 1 Fe unit cell. (a)-(c) Spectra in A_{1g} , B_{2g} , and B_{1g} symmetry. (d) The difference spectra highlight the absence of pair-breaking in B_{2g} and most likely also in A_{1g} symmetry. Only the B_{1g} spectra show the features typical for a superconductor.

the A_{1g} and B_{2g} spectra have edge-like onsets above approximately 150 cm^{-1} before reaching the maxima and decaying slowly. In addition, in either case there are shoulders in the range of 80 cm^{-1} which originate from anisotropies on individual bands and from gaps having different magnitudes on individual bands. The comparison of the spectra in A_{1g} and B_{2g} symmetry and the positions of the B_{1g} collective excitations allow us to pin down the variation of the gaps on the individual bands as shown in Fig. 5 (b).

In contrast to $\text{Rb}_{0.8}\text{Fe}_{1.6}\text{Se}_2$ and $\text{Ba}(\text{Fe}_{0.939}\text{Co}_{0.061})_2\text{As}_2$ (Refs. [20, 27]) gap features are observed in the B_{2g} spectra of $\text{Ba}_{0.6}\text{K}_{0.4}\text{Fe}_2\text{As}_2$. At first glance, this appears to be at odds with the selection rules. However, the outer hole (β) band has a large Fermi momentum $k_F(\beta)$ at which the B_{2g} vertex reaches already 20% of its maximum. In addition, the B_{2g} vertex is enhanced by a factor of approximately 2-5 at the hybridization points of the electron-like γ and δ bands [28]. Therefore, one can see both the small gap of the β band and the large gap on the γ/δ bands at 80 and 210 cm^{-1} , respectively. Apparently, the gap is large at the hybridization points in $\text{Ba}_{0.6}\text{K}_{0.4}\text{Fe}_2\text{As}_2$ as opposed to $\text{Ba}(\text{Fe}_{0.939}\text{Co}_{0.061})_2\text{As}_2$ [20, 28].

DISCUSSION

At this point, a more general picture emerges from the synopsis of the results in $\text{Ba}_{0.6}\text{K}_{0.4}\text{Fe}_2\text{As}_2$, $\text{Ba}(\text{Fe}_{0.939}\text{Co}_{0.061})_2\text{As}_2$, and $\text{Rb}_{0.8}\text{Fe}_{1.6}\text{Se}_2$ with and without central hole bands. In the two extreme cases studied here, we observe more isotropic gaps whereas a strong anisotropy was found in $\text{Ba}(\text{Fe}_{0.939}\text{Co}_{0.061})_2\text{As}_2$ [4, 20] indicating a dramatic change of the pairing potential as predicted in various theoretical studies [29–32].

We now provide evidence for a competition between the two possible pairing states resulting from the exchange of spin fluctuations with V_s and V_d [see Fig. 1(c)] winning in $\text{Ba}_{0.6}\text{K}_{0.4}\text{Fe}_2\text{As}_2$ and $\text{Rb}_{0.8}\text{Fe}_{1.6}\text{Se}_2$, respectively. V_s dominates but V_d is appreciable in $\text{Ba}_{0.6}\text{K}_{0.4}\text{Fe}_2\text{As}_2$ [33]. Then, one expects the system to condense into a ground state having the full symmetry of the lattice and to additionally develop δ -like collective modes with $d_{x^2-y^2}$ orbital momentum bound by the residual interaction V_d inside the gap as shown schematically in Fig. 5(a). Photons ($h\nu$) scatter from both unpaired electrons in the Bogoliubov quasiparticle bands (left) and Cooper pairs at the chemical potential μ (right) [34]. In either case an energy of at least 2Δ must be invested, and an electron-hole pair and two unpaired electrons are created, respectively. The two electrons being separated by 2Δ but remaining in a volume characterized by the coherence length ξ_0 “sense” now those parts of the interaction potential $V_{\mathbf{k},\mathbf{k}'}$ which are orthogonal to the pairing channel and form a bound state of energy E_b inside the gap [9, 11–15]. The δ -like modes appear below the gap edge at $\Omega_b = 2\Delta - E_b$ with E_b being the binding energy of the “Cooperon” [Fig. 5 (a)] [13, 14]. E_b encodes the coupling strength in the subdominant channel and $E_b/2\Delta \approx (V_d/V_s)^2$. The modes at 140, and 175 cm^{-1} correspond to the A_{1g} and B_{2g} gap structures at 190 and 210 cm^{-1} implying binding energies E_b of 50, and 35 cm^{-1} [Fig. 4(b)], respectively, or 25% of 2Δ and indicate that V_d is smaller but of the same order of magnitude as V_s [14]. The bound state at 73 cm^{-1}

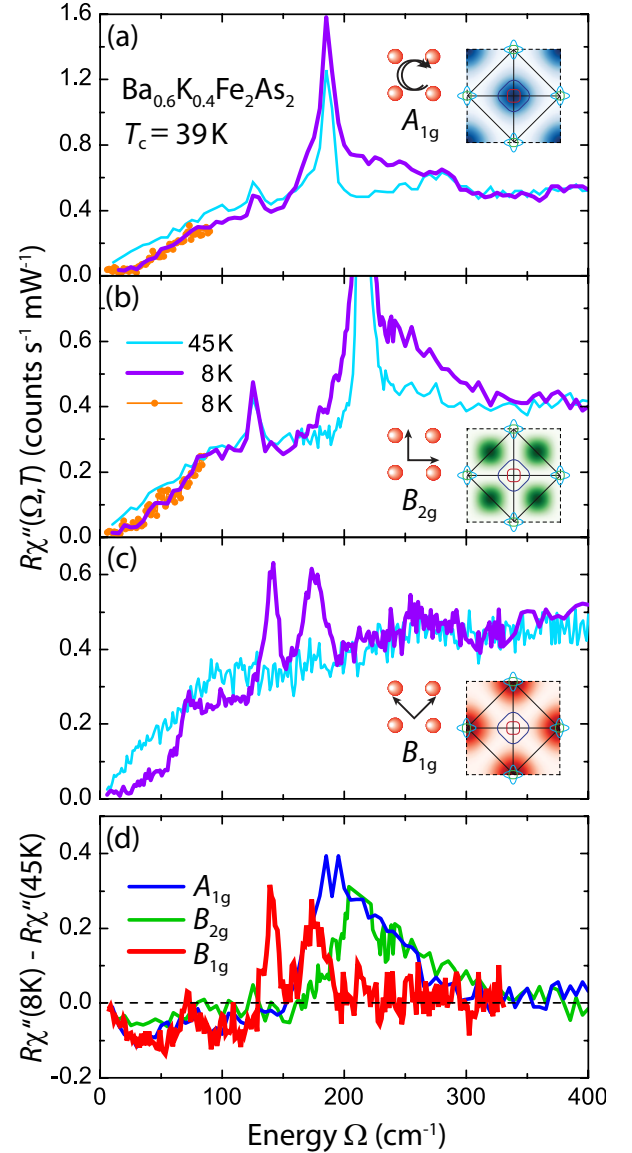


FIG. 4. (Color online) Normal and superconducting Raman spectra of $\text{Ba}_{0.6}\text{K}_{0.4}\text{Fe}_2\text{As}_2$ at temperatures as indicated. The spectra plotted with full lines in panel (a) and (b) are measured with a resolution of 6.5 cm^{-1} whereas the spectra in panel (c) and the spectra displayed with orange points are measured with a resolution of 4.7 cm^{-1} . The insets show the correspondence between light polarizations and sensitivities in momentum space for the 1 Fe unit cell. (a)-(c) Spectra in A_{1g} , B_{2g} , and B_{1g} symmetries. (d) Difference between superconducting and normal-state spectra. In B_{2g} symmetry (green), the phonon at 215 cm^{-1} is truncated.

corresponds to the minimum at 80 cm^{-1} of the strongly momentum dependent gap on the δ band as predicted by Scalapino and Devereaux [9]. This scenario explains in a natural way the two well-defined symmetric peaks at 140 and 175 cm^{-1} and the weaker one at 73 cm^{-1} appearing in (the proper) B_{1g} symmetry [Fig. 4(c) and (d)] and provides direct evidence of a strongly anisotropic pair-

ing potential resulting from a superposition of V_s and V_d . Since the collective modes drain intensity from the gap features [9, 14] direct pair breaking peaks cannot be resolved in B_{1g} symmetry.

Upon going from $\text{Ba}_{0.6}\text{K}_{0.4}\text{Fe}_2\text{As}_2$ to $\text{Ba}(\text{Fe}_{0.939}\text{Co}_{0.061})_2\text{As}_2$ V_d increases becoming comparable to V_s . At first glance the collective modes are expected to become stronger. However, more dramatic changes occur, and the entire pairing state becomes sufficiently anisotropic to drive the minimal gap almost the whole way down to zero at least on portions of the Fermi surface [4, 20]. Now, the collective modes are heavily damped and almost undetectable within experimental uncertainties [9, 35].

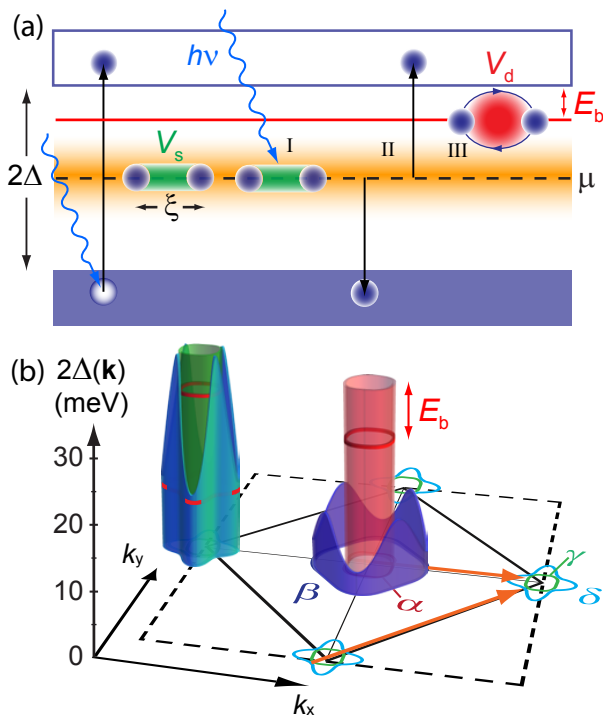


FIG. 5. (Color online) Energy gaps and excitons in superconductors. (a) Mechanism for Bardasis-Schrieffer excitonic modes. (b) Results for the anisotropy of the energy gap in $\text{Ba}_{0.6}\text{K}_{0.4}\text{Fe}_2\text{As}_2$ as derived from Fig. 4. The energy of the bound state E_b (red line) is largest on the α band.

If spin fluctuations dominate the coupling [7] V_s is vanishingly small in $\text{Rb}_{0.8}\text{Fe}_{1.6}\text{Se}_2$ because the central Fermi surface is missing. With V_d surviving alone, the resulting pairing is $d_{x^2-y^2}$ without nodes since the sign change of the gap occurs on the Brillouin zone diagonals far away from the Fermi surface [Fig. 1(f)]. However, after downfolding the 1 Fe Brillouin zone (see Fig. 1) the electron bands accommodating gaps having opposite sign are expected to hybridize. Without mixing of the Cooper pairs on the different bands the gaps have to change sign on the hybridization lines [36]. The resulting nodes on the Fermi surface are incompatible with the observation of a

clean gap [Fig. 3(c)]. If, however, the Cooper pairs can couple across the bands [37] nodeless states can occur again. Our observation of a clean gap in $\text{Rb}_{0.8}\text{Fe}_{1.6}\text{Se}_2$ favors strong hybridization with almost circular concentric Fermi surfaces [37]. As an immediate consequence there is no enhancement of the B_{2g} Raman vertices in $\text{Rb}_{0.8}\text{Fe}_{1.6}\text{Se}_2$ (as opposed to $\text{Ba}_{0.6}\text{K}_{0.4}\text{Fe}_2\text{As}_2$). This explains both the absence of B_{2g} gap features and the clean gap in $\text{Rb}_{0.8}\text{Fe}_{1.6}\text{Se}_2$.

CONCLUSION

The analysis of the Raman results on the gap and of the excitonic in-gap modes of superconducting $\text{Ba}_{0.6}\text{K}_{0.4}\text{Fe}_2\text{As}_2$ provides access to the anisotropy of the pairing potential $V_{\mathbf{k},\mathbf{k}'}$. The dependence of the components V_s and V_d of $V_{\mathbf{k},\mathbf{k}'}$ on the Fermi surface topology makes a strong case for pairing mediated by spin fluctuations. In this way, Raman scattering may well be useful in other circumstances as suggested recently by Barlas and Varma [38] and supplement other methods.

ACKNOWLEDGEMENTS

We gratefully acknowledge discussions with A. Chubukov, T.P. Devereaux, D. Einzel, W. Hanke, A.L. Kemper, I. Mazin, B. Moritz, E.A. Nowadnick, and D.J. Scalapino. R.H. is indebted to the Stanford Institute for Materials and Energy Sciences for the hospitality. We acknowledge support by the DFG under grant number Ha 2071/7 via the Priority Program SPP 1458 as well as TRR 80. The work in China is supported by the NSF of China, the Ministry of Science and Technology of China (973 projects: 2011CBA00102 and 2012CB821403).

-
- [1] W. L. McMillan and J. M. Rowell, *Phys. Rev. Lett.* **14**, 108 (1965).
 - [2] Y. Kamihara, T. Watanabe, M. Hirano, and H. Hosono, *Journal of the American Chemical Society* **130**, 3296 (2008), <http://pubs.acs.org/doi/pdf/10.1021/ja800073m>.
 - [3] M. Rotter, M. Tegel, and D. Johrendt, *Phys. Rev. Lett.* **101**, 107006 (2008).
 - [4] P. J. Hirschfeld, M. M. Korshunov, and I. I. Mazin, *Rep. Prog. Phys.* **74**, 124508 (2011).
 - [5] W.-C. Lee, S.-C. Zhang, and C. Wu, *Phys. Rev. Lett.* **102**, 217002 (2009).
 - [6] R. Thomale, C. Platt, W. Hanke, and B. A. Bernevig, *Phys. Rev. Lett.* **106**, 187003 (2011).
 - [7] I. I. Mazin, D. J. Singh, M. D. Johannes, and M. H. Du, *Phys. Rev. Lett.* **101**, 057003 (2008).
 - [8] H. Kontani and S. Onari, *Phys. Rev. Lett.* **104**, 157001 (2010).

- [9] D. J. Scalapino and T. P. Devereaux, *Phys. Rev. B* **80**, 140512 (2009).
- [10] T. P. Devereaux, *Phys. Rev. B* **50**, 10287 (1994).
- [11] T. P. Devereaux and R. Hackl, *Rev. Mod. Phys.* **79**, 175 (2007).
- [12] A. Bardasis and J. R. Schrieffer, *Phys. Rev.* **121**, 1050 (1961).
- [13] M. V. Klein and S. B. Dierker, *Phys. Rev. B* **29**, 4976 (1984).
- [14] H. Monien and A. Zawadowski, *Phys. Rev. B* **41**, 8798 (1990).
- [15] A. V. Chubukov, I. Eremin, and M. M. Korshunov, *Phys. Rev. B* **79**, 220501 (2009).
- [16] H. Ding, P. Richard, K. Nakayama, K. Sugawara, T. Arakane, Y. Sekiba, A. Takayama, S. Souma, T. Sato, T. Takahashi, Z. Wang, X. Dai, Z. Fang, G. F. Chen, J. L. Luo, and N. L. Wang, *EPL* **83**, 47001 (2008).
- [17] D. V. Evtushinsky, D. S. Inosov, V. B. Zabolotnyy, A. Koitzsch, M. Knupfer, B. Buchner, M. S. Viazovska, G. L. Sun, V. Hinkov, A. V. Boris, C. T. Lin, B. Keimer, A. Varykhalov, A. A. Kordyuk, and S. V. Borisenko, *Phys. Rev. B* **79**, 054517 (2009).
- [18] Y. Zhang, L. X. Yang, M. Xu, Z. R. Ye, F. Chen, C. He, H. C. Xu, J. Jiang, B. P. Xie, J. J. Ying, X. F. Wang, X. H. Chen, J. P. Hu, M. Matsunami, S. Kimura, and D. L. Feng, *Nat Mater* **10**, 273 (2011).
- [19] T. Qian, X.-P. Wang, W.-C. Jin, P. Zhang, P. Richard, G. Xu, X. Dai, Z. Fang, J.-G. Guo, X.-L. Chen, and H. Ding, *Phys. Rev. Lett.* **106**, 187001 (2011).
- [20] B. Muschler, W. Prestel, R. Hackl, T. P. Devereaux, J. G. Analytis, J.-H. Chu, and I. R. Fisher, *Phys. Rev. B* **80**, 180510 (2009).
- [21] B. Shen, H. Yang, Z.-S. Wang, F. Han, B. Zeng, L. Shan, C. Ren, and H.-H. Wen, *Phys. Rev. B* **84**, 184512 (2011).
- [22] V. Tsurkan, J. Deisenhofer, A. Günther, H.-A. Krug von Nidda, S. Widmann, and A. Loidl, *Phys. Rev. B* **84**, 144520 (2011).
- [23] V. Ksenofontov, G. Wortmann, S. A. Medvedev, V. Tsurkan, J. Deisenhofer, A. Loidl, and C. Felser, *Phys. Rev. B* **84**, 180508 (2011).
- [24] A. Charnukha, J. Deisenhofer, D. Pröpper, M. Schmidt, Z. Wang, Y. Goncharov, A. N. Yaresko, V. Tsurkan, B. Keimer, A. Loidl, and A. V. Boris, *Phys. Rev. B* **85**, 100504 (2012).
- [25] Y. Texier, J. Deisenhofer, V. Tsurkan, A. Loidl, D. S. Inosov, G. Friemel, and J. Bobroff, *Phys. Rev. Lett.* **108**, 237002 (2012).
- [26] J. T. Park, G. Friemel, Y. Li, J.-H. Kim, V. Tsurkan, J. Deisenhofer, H.-A. Krug von Nidda, A. Loidl, A. Ivanov, B. Keimer, and D. S. Inosov, *Phys. Rev. Lett.* **107**, 177005 (2011).
- [27] L. Chauvière, Y. Gallais, M. Cazayous, M. A. Méasson, A. Sacuto, D. Colson, and A. Forget, *Phys. Rev. B* **82**, 180521 (2010).
- [28] I. I. Mazin, T. P. Devereaux, J. G. Analytis, J.-H. Chu, I. R. Fisher, B. Muschler, and R. Hackl, *Phys. Rev. B* **82**, 180502 (2010).
- [29] C. Platt, R. Thomale, C. Honerkamp, S.-C. Zhang, and W. Hanke, *Phys. Rev. B* **85**, 180502 (2012).
- [30] K. Kuroki, H. Usui, S. Onari, R. Arita, and H. Aoki, *Phys. Rev. B* **79**, 224511 (2009).
- [31] H. Ikeda, R. Arita, and J. Kuneš, *Phys. Rev. B* **81**, 054502 (2010).
- [32] S. Maiti, M. M. Korshunov, T. A. Maier, P. J. Hirschfeld, and A. V. Chubukov, *Phys. Rev. Lett.* **107**, 147002 (2011).
- [33] R. Thomale, C. Platt, W. Hanke, J. Hu, and B. A. Bernevig, *Phys. Rev. Lett.* **107**, 117001 (2011).
- [34] A. A. Abrikosov and L. A. Fal'kovskii, *Zh. Eksp. Teor. Fiz.* **40**, 262 (1961), [*Sov. Phys. JETP* **13**, 179 (1961)].
- [35] T. P. Devereaux and D. Einzel, *Phys. Rev. B* **51**, 16336 (1995).
- [36] I. I. Mazin, *Phys. Rev. B* **84**, 024529 (2011).
- [37] M. Khodas and A. V. Chubukov, *Phys. Rev. Lett.* **108**, 247003 (2012).
- [38] Y. Barlas and C. M. Varma, arXiv e-prints (2012), [arXiv:1206.0400 \[cond-mat.supr-con\]](https://arxiv.org/abs/1206.0400).